Energy-optimal Speed Trajectories between Stops and Their Parameter Dependence

Eduardo F. Mello[a] and Peter H. Bauer

Department of Electrical Engineering, University of Notre Dame, 275 Fitzpatrick Hall, Notre Dame, U.S.A.

Keywords: Energy, Efficiency, Optimal, Speed Profile, Electric Vehicle.

Abstract: This paper addresses the problem of energy-optimal vehicle-speed trajectories between stops. The ideal parameter-dependent trajectory is introduced, and it is shown that it reduces transportation energy drastically relative to "typical trajectories" seen in traffic. The resulting trajectories can easily be implemented in self-driving cars and have the potential to significantly reduce transportation energy in networked vehicles and cities. The usage of this energy-optimal speed trajectories between stops can save significant amounts of energy, sometimes in excess of 30% when comparing to conventional traffic flow speed profiles. This paper also addresses the impact that vehicle and segment parameters have on the savings. The role of parameters such as the air drag coefficient, cross-sectional area, vehicle mass, efficiency, segment length, average speed, as well as acceleration capability are investigated. It is shown that optimizing speed trajectories to minimize transportation energy consistently results in energy savings. However, diminishing returns are observed for certain scenarios, such as long, low-speed segments.

1 INTRODUCTION

The advent of self-driving cars, intelligent transportation, and connected vehicles opens new possibilities for embedding a variety of algorithms into vehicles that improve and optimize vehicle operations. This is in contrast to the current situation where drivers control vehicle routes and speeds, making the realization of optimization algorithms difficult due to limited acceptance and poor execution by the driver. As shown in (Stern et al., 2018), by adding a sufficient portion of autonomous vehicles executing these embedded algorithms, vehicles that do not use such algorithms could be encouraged or even forced to follow the lead of the self-driven car, at least in dense traffic. This paper explores vehicle-embedded algorithms that minimize energy usage in typical urban driving situations, i.e. from stop to stop. While the approach taken can generally be applied to any type of vehicle, this paper is limited to electric drive systems. The proposed concept minimizes the energy expended at the battery, given the distance and the desired average speed between two stops. Therefore, the algorithm chooses the speed-versus-time trajectory that satisfies the given constraints and minimizes transportation en-

ergy. In order to carry out this type of optimization, one needs to know basic vehicle parameters such as rolling resistance, air drag coefficient, frontal cross-sectional area, vehicle mass, performance limits, and efficiencies along the drivetrain, all parameters that, for a given vehicle, are well known. The optimization algorithm then takes these parameters and the constraints and generates the energy-optimal speed profile. It will be shown that compared to "typical" speed profiles, the optimization results in significant energy savings.

Based on extensive on-road and dynamometer testing, (Hooker, 1988) created guidelines for how a driver should operate a vehicle between consecutive stops; however, in some cases, these guidelines differed significantly, even for similar vehicles. Energy-optimal speed trajectories were also considered for large vehicles. However, the analysis was based on vehicles equipped with internal combustion engines (ICEs) where there is no regenerative braking and the efficiency of the vehicles was not taken into account (Henriksson et al., 2017).

In (Mandava et al., 2009), the authors propose an algorithm that, by using traffic light controller information provided to the vehicle by the roadside, speed recommendations are presented to the driver. The suggested speeds are generated so that the probabil-

---

[a] https://orcid.org/0000-0002-2339-2305

513

ity of green lights when approaching signalized intersections in arterial roads is maximized, resulting in energy savings and reduction of emissions due to the reduction of speed variations and idling times. Addressing a similar problem, (Schuricht et al., 2011) developed an algorithm capable of suggesting the ideal speed profile the driver should adopt in order to cross a traffic light without having to stop to minimize the energy consumption. This research differs from (Mandava et al., 2009) by using information from traffic light controllers and data from a queue length estimator. A slightly different solution was proposed by (Nunzio et al., 2013). Instead of simply avoiding stops in a traffic corridor, the developed algorithm evaluates multiple available no-stop speed profiles and then chooses the most efficient scenario.

With a focus on plug-in hybrid electric vehicles, (Qi et al., 2017) created a system capable of optimizing the speed profile in a signalized arterial road and co-optimizing the vehicle dynamics and hybrid powertrain operations. In a similar approach, the authors in (Barth et al., 2011) calculate the speed profile which minimizes fuel consumption in a signalized arterial road for a vehicle equipped with an internal combustion engine by reducing the total tractive power demand and the idling time.

A separate line of research related to the work proposed in this paper is presented by (Yi and Bauer, 2017b), where the impact of environmental factors such as wind speed, rolling resistance, and temperature on an electric vehicle's energy consumption is analyzed. In (Yi and Bauer, 2018), the authors propose a robust optimization model that exploits these environmental factors to generate an optimal speed profile. Finally, the result in (Yi and Bauer, 2017a) estimates the energy consumption of an electric vehicle based on three parameters (powertrain efficiency, wind speed, and rolling resistance), with variable degree of accuracy depending on energy reserves.

2 THE MODEL

In order to describe the expended energy of a vehicle's speed trajectory, one needs to consider all power-absorbing components, i.e. air drag, rolling resistance, acceleration/deceleration of the vehicle and hill climbing. Therefore, based on the models presented in (Yi and Bauer, 2017b), the power at the wheel, denoted as P_{wheel} can be written as shown in (1) where m, $v(t)$, $\dot{v}(t)$, C_d, and A are the vehicle's mass (which also models and includes the driveline inertia), speed, acceleration, frontal drag coefficient, and cross-sectional area, respectively. ρ is the air density,

f_r is the coefficient of rolling resistance, and g is the gravitational acceleration. In this analysis we assume a flat surface, i.e. no hill climbing.

$$P_{wheel}(t) = mv(t)\dot{v}(t) + \frac{1}{2}C_d A\rho v(t)^3 + mgf_r v(t) \quad (1)$$

The power balance equation for forward motion (2) and for regenerative breaking (3), i.e. reverse power flow, are given by:

$$P_{bat}(t) = \frac{1}{\eta_{frw}}(P_{wheel}(t)) \quad \text{for} \quad P_{wheel} > 0 \quad (2)$$

$$P_{bat}(t) = \eta_{reg}(P_{wheel}(t)) \quad \text{for} \quad P_{wheel} < 0 \quad (3)$$

where $P_{bat}(t)$ is the power at the battery, η_{frw} is the vehicle's efficiency for forward power flow, and η_{reg} is the vehicle's efficiency in reverse power flow. The battery energy, E_{bat}, for the power flow is therefore given by (4).

$$E_{bat} = \int_0^t P_{bat}(t)dt \quad (4)$$

Discretizing the energy equation in (4), a constant approximation can be used for all power absorbing components. The acceleration term is approximated by the difference in kinetic energy values at each distance segment. Each discretized energy segment, ΔE, is described by (5), where v_n denotes a constant-speed segment and Δt a sampling time.

$$\Delta E_n = \frac{m}{2}\left(v_{n+1}^2 - v_n^2\right) + \frac{1}{2}C_d A\rho v_n^3 \Delta t + mgf_r v_n \Delta t \quad (5)$$

The optimization problem can then be formulated in a piecewise discretized form, as shown in (6) and (7). N represents the total number of segments and $\Delta E'$ denotes an energy segment where the forward and reverse power flow efficiencies are accounted for.

$$\Delta E_n' = \begin{cases} \frac{1}{\eta_{frw}}\Delta E_n & for \quad \Delta E > 0 \\ \eta_{reg}\Delta E_n & for \quad \Delta E \leq 0 \end{cases} \quad (6)$$

$$E = \sum_{n=1}^{N} \Delta E_n' \quad (7)$$

Finally, the optimization problem can then be written as shown in (8).

$$\min_{v_n} E$$

$$s.t. \sum_{n=1}^{N} \frac{v_n}{N} = v_{avg}$$

$$0 \leq v_n \leq v_{max}$$

$$d_{max} \leq \frac{v_{n+1} - v_n}{\Delta t} \leq a_{max} \ \forall \ n \in \{1, ..., N-1\}$$

$$d_{max} \leq \frac{-v_n}{\Delta t} \leq a_{max} \qquad if \ n = N$$

$$(8)$$

where v_{avg} is the desired average speed, v_{max} is the maximum allowed speed, d_{max} is the maximum allowable deceleration, and a_{max} is the maximum allowable acceleration.

3 SIMULATION RESULTS AND OPTIMIZATION

The optimization problem expressed in (8) was implemented using the *fmincon* solver from MATLAB with the *Sequential Quadratic Programming (SQP)* algorithm. In order to verify if the optimization proposed in this paper would be applicable to various vehicles and scenarios, a number of simulations with different parameter sets were performed. Initially, a short segment was tested with two vehicle models, one based on a Nissan Leaf and the second based on a Tesla Model S. Then, parameters such as average speed of the vehicle, segment length, maximum tolerable accelartions and decelerations, and the vehicle efficiency were varied. Finally a larger sample of vehicles in a number of different scenarios were tested.

3.1 Approximation of a Real Scenario

In order to define a baseline for typical traffic flow, the Federal Test Procedure (FTP-75) drive cycle was analyzed. To generate the typical traffic profile the drive cycle was divided into segments (corresponding to the periods for which the car is movement), normalized in time and speed, and then all segments were averaged.

The curve generated was then approximated by an exponential acceleration until it reached the maximum speed followed by a parabolic deceleration. Both curves are shown in Figure 1 where the curve "Real scenario" is extracted from the FTP-75 drive cycle and the curve "Typical traffic" shows the approximated curve.
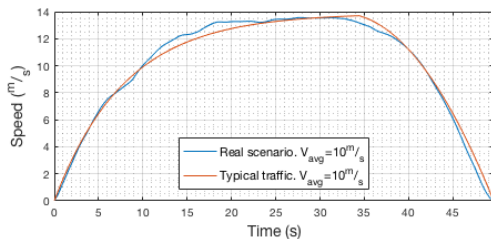

Figure 1: Speed vs. time of the "Real scenario" extracted from FTP-75 and approximated "Typical traffic" flow.

3.2 Optimization Results for Urban Traffic

The proposed optimization was used for a couple of vehicles in order to verify the robustness of the results relative to vehicle and infrastructure parameters. The first tested case was for a vehicle with a parameter set based on a Nissan Leaf in a 300-meter segment. The second vehicle model utilized was based on a Tesla Model S in a segment with the same 300-meter in length.

3.2.1 Nissan Leaf

The baseline case is investigated for a midsize electric vehicle (EV), which has its parameter set based on the Nissan Leaf. The vehicle data set is given as follows: $m = 1525 kg$, $f_r = 0.01$, $C_d = 0.29$, and $A = 2.27 m^2$. The average forward and reverse power flow efficiencies were approximated as $\eta_{frd} = 0.7$, and $\eta_{reg} = 0.2$.

The speed trajectories for the approximation of the typical traffic flow and the optimized trajectory are shown in Figure 2. Figure 3 shows the acceleration profile necessary to realize the aforementioned speed profiles. And finally, the energy utilized by the vehicle in each case is shown Figure 4.

In this simulation, the constraints imposed on the optimizer were: the length between two consecutive stops was chosen to be $300m$, the average speed throughout the profile had to be equal to $10m/s$, the maximum acceleration $4.6m/s^2$, the maximum deceleration $-2m/s^2$, and finally, the initial and final speeds equal to zero.

The results obtained show that the optimized speed profile consumes $179.9kWs$ while the typical traffic baseline uses $235.4kWs$, a 23.59% reduction. This demonstrates that the optimization proposed in this paper has the potential of drastically minimizing the energy consumption in a route with necessary stops.

3.2.2 Tesla Model S

The optimization was then repeated for a vehicle with a parameter set based on the Tesla Model S. This vehicle was chosen as it is another typical electric vehicle and it has higher maximum acceleration and deceleration than a Nissan Leaf. The parameter values utilized are: $m = 2018kg$, $f_r = 0.01$, $C_d = 0.24$, and $A = 2.8m^2$. The average forward and reverse power flow efficiencies were approximated as $\eta_{frd} = 0.7$, and $\eta_{reg} = 0.2$. The distance between the two stops was kept at $300m$. The acceleration of the vehicle was limited to $8m/s^2$ and the deceleration to $-2.5m/s^2$.
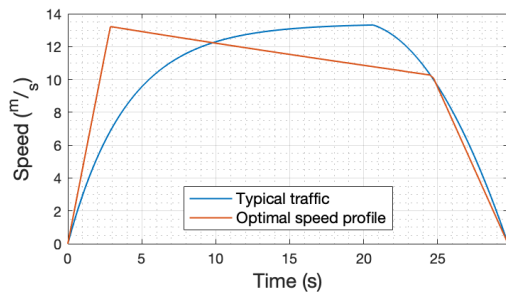
Figure 2: Speed for the "Typical traffic" and "Optimal speed" profiles for a Nissan Leaf.
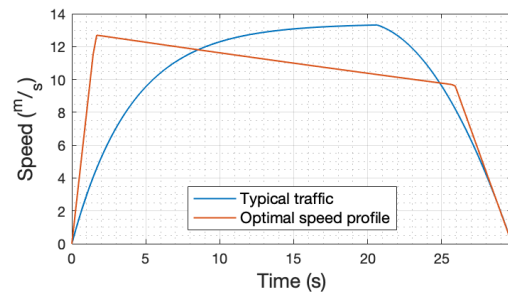

Figure 3: Acceleration for the "Typical traffic" and "Optimal speed" profiles for a Nissan Leaf.

Figure 4: Energy for the "Typical traffic" and "Optimal speed" profiles for a Nissan Leaf.

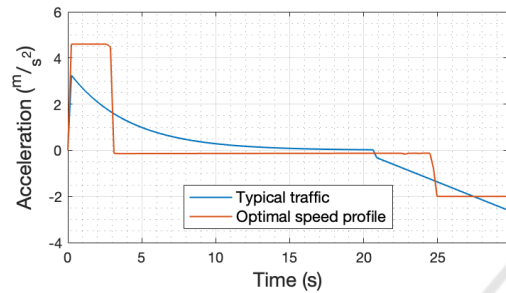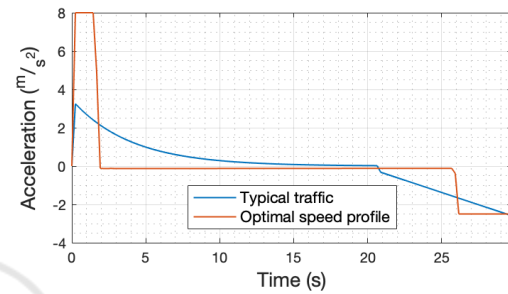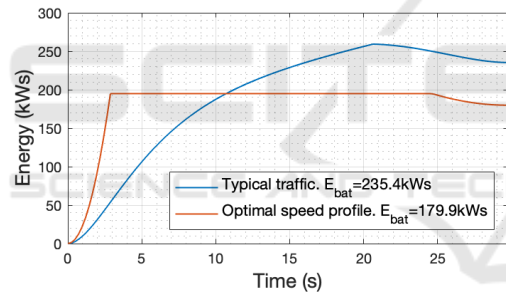Figure 5: Speed for the "Typical traffic" and "Optimal speed" profiles for a Tesla Model S.

Figure 6: Acceleration for the "Typical traffic" and "Optimal speed" profiles for a Tesla Model S.
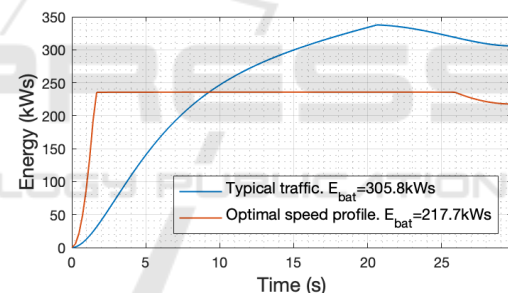

Figure 7: Energy for the "Typical traffic" and "Optimal speed" profiles for a Tesla Model S.

As already seen in Figure 2, the optimal speed profile for this vehicle, Figure 5, is characterized by three different stages (acceleration, coasting, and deceleration) until a complete stop is reached. With the aforementioned parameters, the optimizer produced a speed profile which uses $217.7kWs$, as seen in Figure 7. This value is 28.81% less than the one obtained for the typical traffic baseline, which used $305.8kWs$, saving $88.1kWs$.

As expected, since the Tesla Model S is a heavier vehicle with a larger cross-sectional area, it uses more energy than the Nissan Leaf in each of the driving schedules, i.e. typical traffic baseline and optimal speed profile. However, the Tesla Model S was able to achieve greater percentage savings when compared to the Nissan Leaf due to its greater acceleration and deceleration.

3.3 The Effects of Segment Length and Average Speed

Two simulations were performed in order to verify the effects of average speed and segment length in the optimized speed profiles. Both simulations were performed for the same vehicle with parameters based on a Tesla Model S.

3.3.1 Midrange Segment Length and High Speed

The initial scenario simulated was a segment of $1000m$ at an average speed of $20m/s$. The stop-to-stop length and average speed were chosen in order to keep the accelerations and decelerations in our baselines within realistic margins. One important aspect
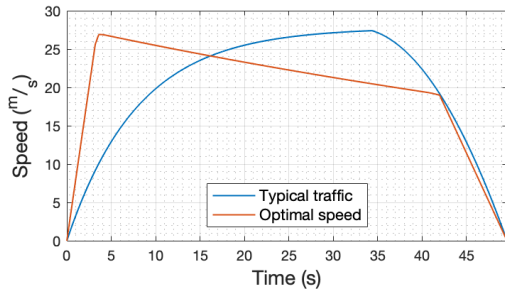
Figure 8: Speed for "Typical traffic" and "Optimal speed" profiles for a stop-to-stop segment length of 1000*m* and average speed of 20*m/s*.
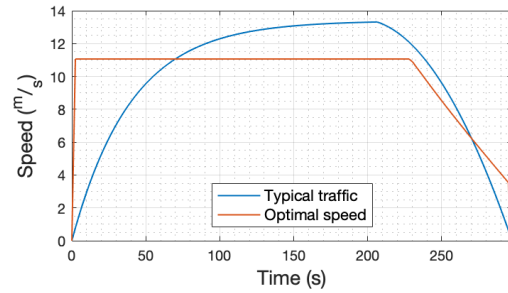

Figure 10: Speed for "Typical traffic" and "Optimal speed" profiles for a stop-to-stop segment length of 3000*m* and average speed of 10*m/s*.
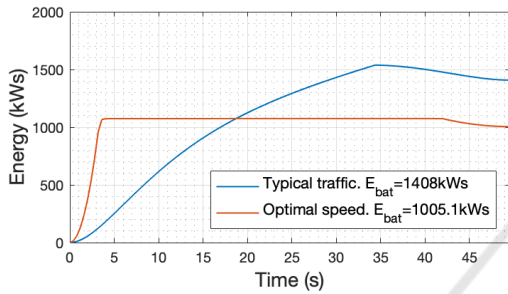

Figure 9: Energy for "Typical traffic" and "Optimal speed" profiles for a stop-to-stop segment length of 1000*m* and average speed of 20*m/s*.
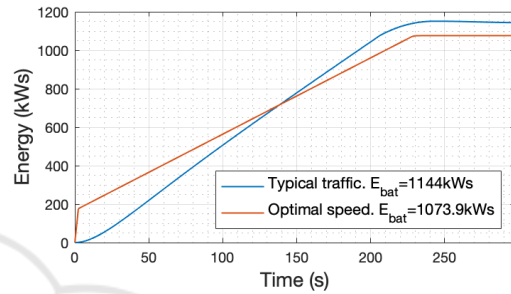

Figure 11: Energy for "Typical traffic" and "Optimal speed" profiles for a stop-to-stop segment length of 3000*m* and average speed of 10*m/s*.

to be kept in mind is that the speed profile baselines must have realizable accelerations in order to be compared to the results of the optimizer, which has realizable accelerations as constraints. In this case, as shown in Figures 8 and 9, it was observed that the optimized speed profile saves 402.9*kWs* when compared to the typical traffic baseline, which is equivalent to 28.61%. The total energy used in the simulation was 1408*kWs* for the baseline and 1005.1*kWs* for the optimal speed profile. Based on these results, it is clear that the optimizer is capable of generating significant savings even for higher speed scenarios.

3.3.2 Long Segment Length and Low Speed

Figures 10 and 11 show the simulation for a segment length of 3000*m* at a speed of 10*m/s*, i.e. half of the speed used in the previous case. The results obtained from the optimizer show savings of 6.13% when compared to the typical traffic baseline. This value corresponds to 70.14*kWs*. With the information provided by this simulation, it can be concluded that this optimization has diminished results when the length of the stop-to-stop segment is drastically increased.

3.4 The Effects of Maximum Tolerable Acceleration and Deceleration

As seen in Figure 8 and Figure 10, the optimal speed profile is typically characterized by three to four pronounced segments: acceleration, constant speed (which in certain circumstances may not exist), coasting, and deceleration. These well-defined segments raise the question of what the effects of the acceleration and deceleration limits (constraints of the optimizer) are.

To verify the effects of the aforementioned limits, the simulation in section 3.2.2 was repeated with new limits for the acceleration and deceleration constraints. The segment length was kept at 300*m* with an average speed of 10*m/s*. The acceleration of the vehicle was limited to 4*m/s²* and the deceleration to -1.25*m/s²*. These values correspond to half of the ones used in section 3.2.2. With these parameters, the optimizer produced a speed profile which uses 274.4*kWs*. This value is 10.44% smaller than the one obtained for the typical traffic baseline, saving 31.98*kWs*. The optimal speed profile generated can be seen in Figures 12 and 13.

In this simulation, the acceleration and deceleration limits were set to half of the values utilized in section 3.2.2. This change caused an increase in energy
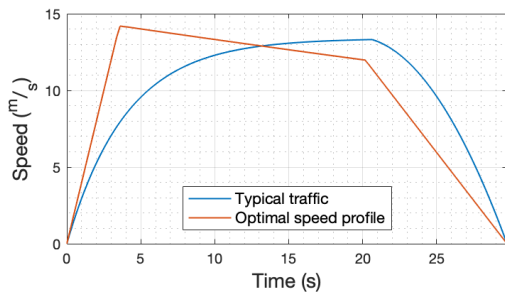
517

Figure 12: Speed for the "Typical traffic" and "Optimal speed" profiles for a Tesla Model S with reduced maximum acceleration and deceleration in a 300-meter segment.

Figure 13: Energy for the "Typical traffic" and "Optimal speed" profiles for a Tesla Model S with reduced maximum acceleration and deceleration in a 300-meter segment.
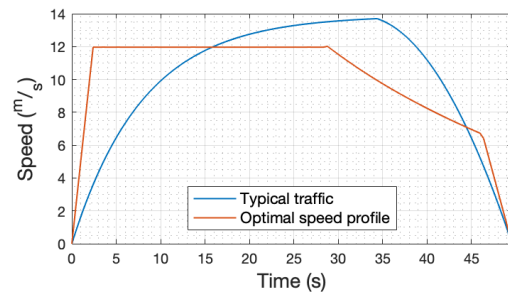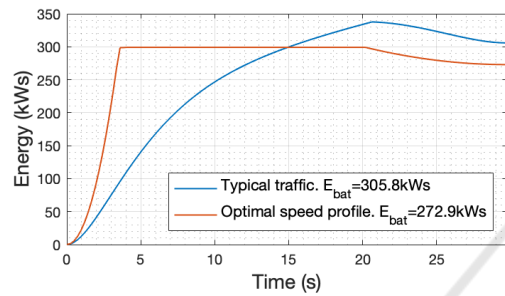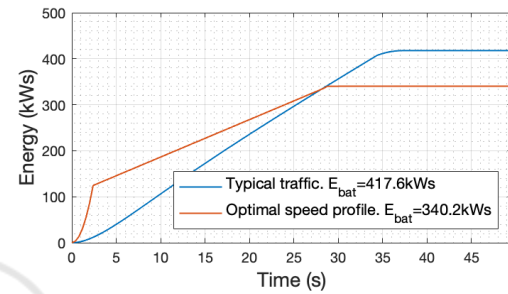
consumption of $55.2kWs$. This energy increase corresponds to 18.37% of the energy utilized by the vehicle when higher acceleration and deceleration were allowed. Thus, it can be stated that by increasing the maximum tolerable acceleration and deceleration, higher savings can be achieved.

3.5 The Effects of Vehicle Efficiency

3.5.1 Highly Inefficient Vehicle

In order to validate the robustness of the results with respect to the vehicle model, another set of simulations was run. The first simulation represents a highly inefficient vehicle with the following parameters: $m = 1000kg$, $f_r = 0.015$, $C_d = 1$, and $A = 3m^2$, $\eta_{frd} = 0.6$, and $\eta_{reg} = 0$. The acceleration was limited to $5m/s^2$ and the deceleration to $-2m/s^2$. The segment length was set to $500m$ with an average speed of $10m/s$.

The simulation output showed a significant improvement over the speed profile baselines for the inefficient vehicle, as seen in Figures 14 and 15. The optimized speed profile was able to save $77.4kWs$ over the typical traffic flow baseline, which corresponds to 18.52% of improvement. Therefore, the algorithm showed to be a very plausible option for reducing the energy consumption of highly inefficient electric vehicles.

Figure 14: Speed for the "Typical traffic" and "Optimal speed" profiles for a highly inefficient vehicle.

Figure 15: Energy for the "Typical traffic" and "Optimal speed" profiles for a highly inefficient vehicle.

3.5.2 Highly Efficient Vehicle

The second simulation assumes a model of a highly efficient vehicle. Its parameters were defined as: $m = 2000kg$, $f_r = 0.008$, $C_d = 0.25$, $A = 2m^2$, $\eta_{frd} = 0.9$, and $\eta_{reg} = 0.5$. The acceleration was once again limited to $5m/s^2$ and the deceleration to $-2m/s^2$. The segment length and average speed were also kept the same—$500m$ and $10m/s$.

With the parameters described above, drops in energy consumption of 26.73% with respect to the typical traffic baseline were observed (Figures 16 and 17). These savings correspond to $56.29kWs$. Thus, it can be assumed that the optimization is capable of significant energy savings for efficient and inefficient electric vehicles, where greater savings are observed for an efficient vehicle.

3.6 Additional Vehicle Models and the Impact of the Segment Length

A final set of simulations was performed in order to compare a number of different scenarios where the vehicle parameters, segment length, and average speed were varied. Five vehicle parameter sets were utilized and they are specified in Table 1. Vehicle type 1 has a parameter set similar to the parameters of a Tesla Model S and vehicle type 2 has similar parameters to a Nissan Leaf. Parameters such as vehicle
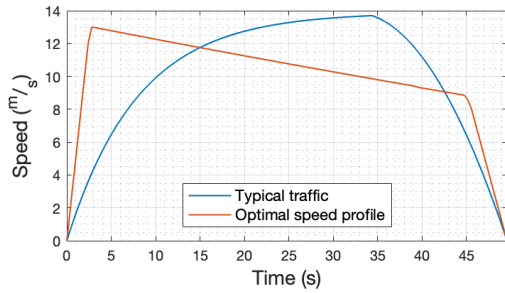
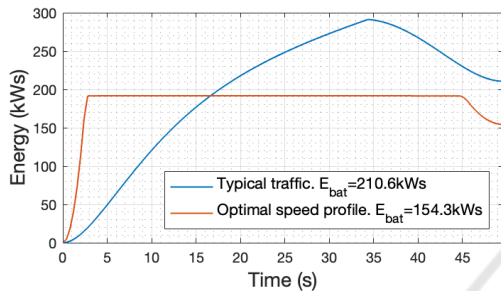Figure 16: Speed for the "Typical traffic" and "Optimal speed" profiles for a highly efficient vehicle.

Figure 17: Energy for the "Typical traffic" and "Optimal speed" profiles for a highly efficient vehicle.

mass, cross-sectional area multiplied by air drag coefficient, efficiencies, and maximum acceleration and deceleration were modified in order to analyze the impact they have on transportation energy savings. Vehicle type 3 is a variation of vehicle type 2 with high maximum acceleration and deceleration. Vehicle types 4 and 5 have extreme parameter sets with high mass and low Cd_A for the former and low mass and high Cd_A for the latter to illustrate the effects of these vehicle parameters.

Table 1: Vehicle parameters utilized in simulations.

Vehicle	Mass (kg)	C_dA (m^2)	Max. acceler. (m/s^2)	Max. deceler. (m/s^2)
Type 1	2,018	0.6720	8	2.5
Type 2	1,525	0.6583	4.6	2
Type 3	1,525	0.6583	8	2.5
Type 4	2,500	0.5	4.6	2
Type 5	800	2.0	4.6	2

A segment length of 300 meters was used in most simulations since it is a typical length for a suburban block (Hooker, 1988).

Table 2 shows the results obtained. In all cases, the optimal trajectory results in energy savings. These savings demonstrate the robustness of the optimization results with respect to the vehicle parameter set. However, the segment length has a significant impact

on energy savings. Improvements ranging from 6% to 41% were observed in this set of simulations.

These results show that energy savings are particularly high for short distance segments. Also, vehicles capable of accelerating rapidly have greater savings in transportation energy, which is especially pronounced in short segments. This can be seen by noticing that Vehicle type 3 obtains higher savings than Vehicle type 2 (mostly identical vehicles with exception of the acceleration capabilities). Also, Vehicle type 1 obtained higher savings than Vehicle type 2 in almost all scenarios. Finally, it can be observed that high savings are also obtained for vehicles traveling at higher average speeds in long segments.

4 CONCLUSIONS

This paper shows that optimized speed trajectories between stops can lead to significant transportation-energy savings. Depending on the distance, average speed, and vehicle parameters, energy savings can reach approximately 40% relative to typically seen speed profiles. It is important to note that savings are dependent on the speed profile used as the baseline. It was further shown that the optimal speed profile usually has three to four distinct segments: acceleration, constant speed (which is not present for short distances), coasting, and deceleration. All speed trajectories show the same trend regardless of the parameter set: the more energy that can be expended at the beginning of the stop-to-stop segment, the higher the savings.

In addition, this paper examined the effects of different vehicle parameters and operating conditions on transportation energy savings relative to conventional stop-to-stop speed trajectories. In all cases, the optimal trajectory results in energy savings, which in the simulations presented in this paper range from 6% to 41%, depending on the constraints and parameters chosen. This is only possible due to the robust nature of the optimization results obtained with respect to vehicle and infrastructure parameters. Energy savings are particularly high for short distance segments. Also, vehicles capable of accelerating rapidly have greater savings in transportation energy, which is especially pronounced in short segments.

Therefore, the impact on self-driving electric vehicles (EVs) and the associated transportation infrastructure is twofold: range improvement of EVs due to lower energy expenditure in urban driving situations, and less power demand from the grid to charge EVs. It is important to note that the speed controller that executes the optimal trajectory needs to communicate

Table 2: Energy consumption for different vehicles and segment lengths.

Vehicle	Forward Power Flow Efficiency	Reverse Power Flow Efficiency	Average speed (m/s)	Segment length (m)	Energy utilized		Energy saved
					Typical trajectory (kWs)	Optimal trajectory (kWs)	
Vehicle type 1	0.7	0.2	10	300	305.8	217.7	28.81 %
				500	375.4	253.7	32.42 %
				1,000	519.7	393.7	24.24 %
				3,000	1,144.0	1,073.9	6.13 %
			18	3,000	2,043.7	1,643.8	19.57 %
Vehicle type 2	0.7	0.2	10	300	235.4	179.9	23.59 %
				500	290.9	203.9	29.91 %
				1,000	407.7	314.4	22.88 %
				3,000	915.1	853.8	6.7 %
			18	3,000	1,695.7	1,392.7	17.87 %
Vehicle type 3	.7	.2	10	300	235.4	167.9	28.67 %
Vehicle type 4					449.2	291.9	35.02 %
Vehicle type 5					234.0	137.6	41.20 %

with the self-driving software in order to prevent accidents. Even though the proposed speed trajectories have strong accelerations, the speeds in urban scenarios are generally around 50km/h or less.

REFERENCES

Barth, M., Mandava, S., Boriboonsomsin, K., and Xia, H. (2011). Dynamic eco-driving for arterial corridors. In *2011 IEEE Forum on Integrated and Sustainable Transportation Systems*, pages 182–188.

Henriksson, M., Flärdh, O., and Mårtensson, J. (2017). Optimal speed trajectories under variations in the driving corridor. *IFAC-PapersOnLine*, 50(1):12551 – 12556. 20th IFAC World Congress.

Hooker, J. (1988). Optimal driving for single-vehicle fuel economy. *Transportation Research Part A: General*, 22(3):183 – 201.

Mandava, S., Boriboonsomsin, K., and Barth, M. (2009). Arterial velocity planning based on traffic signal information under light traffic conditions. In *2009 12th International IEEE Conference on Intelligent Transportation Systems*, pages 1–6.

Nunzio, G. D., de Wit, C. C., Moulin, P., and Domenico, D. D. (2013). Eco-driving in urban traffic networks using traffic signal information. In *52nd IEEE Conference on Decision and Control*, pages 892–898.

Qi, X., Wu, G., Hao, P., Boriboonsomsin, K., and Barth, M. J. (2017). Integrated-connected eco-driving system for phevs with co-optimization of vehicle dynamics and powertrain operations. *IEEE Transactions on Intelligent Vehicles*, 2(1):2–13.

Schuricht, P., Michler, O., and Bäker, B. (2011). Efficiency-increasing driver assistance at signalized intersections using predictive traffic state estimation. In *2011 14th International IEEE Conference on Intelligent Transportation Systems (ITSC)*, pages 347–352.

Stern, R. E., Cui, S., Monache, M. L. D., Bhadani, R., Bunting, M., Churchill, M., Hamilton, N., Haulcy, R., Pohlmann, H., Wu, F., Piccoli, B., Seibold, B., Sprinkle, J., and Work, D. B. (2018). Dissipation of stop-and-go waves via control of autonomous vehicles: Field experiments. *Transportation Research Part C: Emerging Technologies*, 89:205 – 221.

Yi, Z. and Bauer, P. H. (2017a). Adaptive multiresolution energy consumption prediction for electric vehicles. *IEEE Transactions on Vehicular Technology*, 66(11):10515–10525.

Yi, Z. and Bauer, P. H. (2017b). Effects of environmental factors on electric vehicle energy consumption: a sensitivity analysis. *IET Electrical Systems in Transportation*, 7(1):3–13.

Yi, Z. and Bauer, P. H. (2018). Energy aware driving: Optimal electric vehicle speed profiles for sustainability in transportation. *IEEE Transactions on Intelligent Transportation Systems*, pages 1–12.